

Sensitivity of Ozone to Bromine in the Lower Stratosphere

R.J. Salawitch¹, D.K. Weisenstein², L.J. Kovalenko³, C.E. Sioris⁴, P.O. Wennberg³, K. Chance⁴, M.K.W. Ko⁵, C.A. McLinden⁶

[1] Measurements of BrO suggest that inorganic bromine (Br_y) at and above the tropopause is 4 to 8 ppt greater than assumed in models used in past ozone trend assessment studies. This additional bromine is likely carried to the stratosphere by short-lived biogenic compounds and their decomposition products, including tropospheric BrO. Including this additional bromine in an ozone trend simulation increases the computed ozone depletion over the past ~25 years, leading to better agreement between measured and modeled ozone trends. This additional Br_y (assumed constant over time) causes more ozone depletion because associated BrO provides a reaction partner for ClO, which increases due to anthropogenic sources. Enhanced Br_y causes photochemical loss of ozone below ~14 km to change from being controlled by HO_x catalytic cycles (primarily $\text{HO}_2 + \text{O}_3$) to a situation where loss by the $\text{BrO} + \text{HO}_2$ cycle is also important.

1. Introduction

[2] Models used to quantify our understanding of ozone trends rely on estimates of stratospheric inorganic bromine (Br_y) based on the decomposition of the long-lived source gases methyl bromide (CH_3Br) and halons in the stratosphere [WMO, 2003]. For the assumed sources, the abundance of Br_y calculated in these models is close to zero at the tropopause, increasing with altitude as air photochemically ages.

[3] There have been many suggestions that non-zero levels of Br_y exist near the tropopause [e.g., chapter 2 of WMO 2003]. Possible contributions to Br_y from decomposition of short-lived halogens such as CHBr_3 , CH_2BrCl , CHBrCl_2 , $\text{CH}_2\text{BrCH}_2\text{Br}$ [Wamsley *et al.*, 1998; Dvortsov *et al.* 1999; Schauffler *et al.* 1999; Sturges *et al.*, 2000] or the transport of BrO across the tropopause [Ko *et al.*, 1997; Pfeilsticker *et al.*, 2000] have been described. Estimates of upper stratospheric Br_y from balloon-borne observations of BrO are 6 ppt larger than the expected bromine content based on measurements of CH_3Br +halons [figure 1-8, WMO 2003].

[4] We present observations of BrO that suggest Br_y near the tropopause (termed $\text{Br}_y^{\text{TROP}}$) might be as high as 4 to 8 ppt. Possible source species are described. We quantify the effect of excess bromine in the lowermost stratosphere (LMS) on the photochemical budget and trends of ozone by increasing Br_y , within the AER 2D model, by specified amounts relative to abundances found using the WMO [2003] Ab baseline scenario for organic bromine source gases.

2. The Bromine Budget

[5] Measurements of total column BrO from space reveal much higher abundances than found from standard stratospheric models. The vertical column of BrO from GOME [Chance, 1998] during May 1997 far exceeds vertical BrO columns from the AER model (auxiliary material¹). Much attention has focused on whether this discrepancy might be explained by a global, ubiquitous background level of 1 to 2 ppt of BrO in the free troposphere [Platt and Hönniger, 2003]. However, an examination of ground-based diffuse and direct sunlight over Lauder, NZ (45°S) indicates a mean value for tropospheric BrO of 0.2 ppt and an upper limit of 0.9 ppt [Schofield *et al.*, 2004].

[6] Inconsistencies between stratospheric Br_y inferred from BrO and the delivery of bromine to the stratosphere by long-lived organic source molecules are indicated by data shown in figure 7 of Wamsley *et al.* [1998]. A photochemical model was used to compute Br_y from in situ aircraft observations of BrO in the LMS. For our Figure 1 we have taken those data from Wamsley *et al.* [1998] and added vertical error bars to represent a root-sum-of-squares (RSS) combination of the 2σ uncertainties in the BrO measurement and uncertainties in the computation of Br_y from BrO; horizontal error bars denote the standard deviation of measured CFC-11 (a tracer of photochemical aging) during the time the BrO data were obtained. Figure 1a compares Br_y derived from BrO to estimates of stratospheric bromine from the Wamsley organic relation, which assumes contributions to Br_y from CH_3Br , halons, CH_2Br_2 and CH_2BrCl . Also shown are estimates of Br_y found by applying $\text{Br}_y^{\text{TROP}}$ offsets of 4 and 8 ppt to the Wamsley relation. This comparison suggests the 6 organic compounds considered by Wamsley do not supply the full burden of stratospheric Br_y .

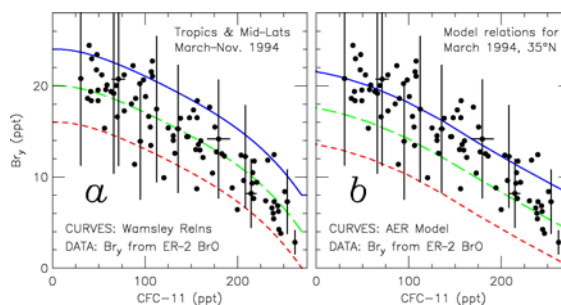


Figure 1a. Calculated Br_y from in situ BrO (data points; see text for error bar description) plotted versus CFC-11 compared to the estimate of Br_y from measurements of the decomposition of CH_3Br , H-1211, H-1301, H-2402, CH_2Br_2 , and CH_2BrCl (red short-dashed) given by Wamsley *et al.* [1998]. Also shown are estimates of Br_y from organics for $\text{Br}_y^{\text{TROP}}$ of 4 ppt (green long-dashed) and 8 ppt (blue solid). **Panel b.** Same as panel a, except Br_y is from the AER 2D model for 35°N, Sept. 1994, using source gases CH_3Br , H-1211, H-1301, H-2402, and H-1202 as described by the WMO Ab baseline scenario.

¹Jet Propulsion Laboratory, California Institute of Technology, Pasadena, CA

²Atmospheric and Environmental Research, Inc, Lexington, MA

³California Institute of Technology, Pasadena, CA

⁴Harvard-Smithsonian Center for Astrophysics, Cambridge, MA

⁵NASA Langley Research Center, Hampton, VA

⁶Meteorological Service of Canada, Toronto, Canada

[7] Figure 1b presents a similar comparison for Br_y from the AER model. This plot indicates the bromine content of the stratosphere is much larger than within the model for the WMO Br_y scenario (differences quantified in auxiliary material¹). The discrepancy is larger than found for the Wamsley relation because the WMO scenario neglects contributions to Br_y from CH_2Br_2 and CH_2BrCl . These short-lived biogenic compounds deliver ~ 2.3 ppt of bromine to the LMS [Wamsley *et al.*, 1998].

[8] The only published profile of BrO in the tropics (22°S, Nov. 1997) indicates the presence of significant levels of BrO in the upper troposphere [Pundt *et al.*, 2002]. We have calculated Br_y from these balloon-borne, spectroscopic measurements of BrO as described in the auxiliary material¹. The resulting profile of Br_y is much larger than found within the AER model using the WMO Br_y scenario (Figure 2). The inferred Br_y profile suggests the conversion of organic bromine to inorganic forms below the tropopause, as noted by Pundt *et al.* [2002]. At higher altitudes, empirical Br_y is considerably larger than Br_y based solely on supply from CH_3Br +halons. This analysis suggests the contribution to Br_y from other species is ~ 8 ppt or perhaps larger. Also, vertical profiles of BrO retrieved from limb scatter radiances acquired by SCIAMACHY, between latitudes of 70°S and 60°N, indicate both the presence of significant levels of Br_y near the tropopause and a budget for middle stratospheric Br_y consistent with $\text{Br}_y^{\text{TROP}} \approx 8$ ppt [Sioris *et al.*, manuscript in preparation].

[9] We return to the GOME observations of column BrO. Figure 3 shows the estimated stratospheric contribution to the BrO column measured by GOME, if 1 ppt of BrO had been uniformly distributed throughout the troposphere (1 ppt tropos. BrO \approx

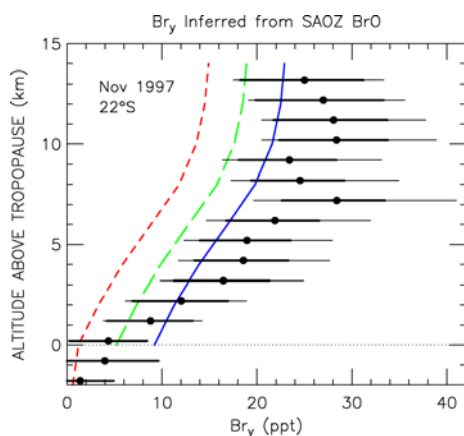


Figure 2. Profile of Br_y inferred from SAOZ BrO [Pundt *et al.*, 2002] at 22°S, Nov 1997 compared to profiles from the AER model for 20°S, Nov. 1997 using $\text{Br}_y^{\text{TROP}}$ of 0, 4, and 8 ppt (same line types as Fig. 1). Profiles are plotted relative to the local tropopause of measurement (16.8 km) and model (16.0 km). Thick error bars denote 1σ uncertainty in Br_y due just to the total measurement uncertainty for BrO. Thin error bars denote the overall 1σ uncertainty for Br_y , found from a RSS combination of the kinetic uncertainties involved in computing Br_y from BrO and the measurement uncertainty for BrO. At the lowest altitudes, overall uncertainty is dominated by the BrO measurement precision and the thin and thick error bars completely overlap. Details of the inferred Br_y calculation are given in the auxiliary material¹.

2.2×10^{13} #/cm² at 35°N; details and discussion of “Enhanced Tropospheric BrO” feature in auxiliary material¹). Figure 3 suggests an overall level of consistency can be achieved between satellite measurements of total BrO, aircraft and satellite measurements of stratospheric BrO, and ground-based upper limits for tropospheric BrO assuming both a stratospheric ($\text{Br}_y^{\text{TROP}}$ of 4 to 8 ppt) and tropospheric contribution (1 ppt) to the high values of BrO measured by GOME.

[10] Numerous very-short lived (VSL) compounds likely contribute to Br_y at the tropical tropopause [WMO, 2003]. Bromoform (CHBr_3) levels as high as 1 ppt exist in the tropical mid-troposphere [Schauffler *et al.*, 1999; Sturges *et al.*, 2000] and this compound has the capacity to increase Br_y in the LMS by ~ 2 ppt [Dvortsov *et al.*, 1999]. Ethylene dibromide ($\text{C}_2\text{H}_4\text{Br}_2$) has been measured to be ~ 1 ppt at the South Pole [Khalil and Rasmussen, 1985] and ~ 5.0 ppt in urban areas [Pratt *et al.*, 2000], has anthropogenic sources [Khalil and Rasmussen, 1985], and has the potential to deliver significant amounts of Br_y to the tropopause. Decomposition products from $\text{C}_2\text{H}_5\text{Br}$, CHBr_2Cl , and $\text{C}_3\text{H}_7\text{Br}$ provide a possible additional contribution of ~ 0.7 ppt to $\text{Br}_y^{\text{TROP}}$ [Pfeilsticker *et al.*, 2000; WMO, 2003]. These abundances, combined with the 2.3 ppt from CH_2Br_2 and CH_2BrCl and the possible ~ 1 to 2 ppt background BrO (albeit, this might be supplied by the above mentioned species), are consistent with our 4 to 8 ppt estimate for $\text{Br}_y^{\text{TROP}}$ based on measured BrO.

[11] The mechanism for supply of Br_y to the tropopause requires further study. Since HBr and HOBr are soluble, we might expect inorganic species produced by the decomposition of VSL biogenic compounds to rain out before reaching the stratosphere. However, heterogeneous reactions on tropospheric aerosol might liberate bromine back to the gas phase, allowing for delivery of Br_y derived from these organic compounds to the stratosphere [Platt and Hönninger, 2003].

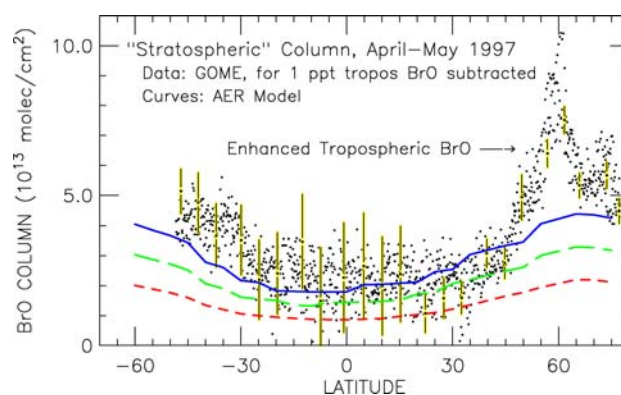


Figure 3. Estimated stratospheric BrO column from GOME for May 2, 1997 assuming a 1 ppt, uniform distribution of BrO in the troposphere [close to the upper limit of 0.9 ppt reported by Schofield *et al.*, 2004] compared to the stratospheric column from the model (mid-April, 1997), found by integrating above a chemical tropopause defined by the $\text{O}_3=0.1$ ppm level, for $\text{Br}_y^{\text{TROP}}$ of 0, 4, and 8 ppt. Error bars (1σ total uncertainty) [Chance, 1998] are shown every 50th point, for clarity. All data and model results are restricted to $\text{SZA} < 70^\circ$ so that diurnal variation of the BrO column cannot be responsible for any significant portion of the model-measurement differences.

[12] Many prior studies have examined the bromine budget. *Avallone et al.* [1995] used airborne observations of BrO and organic source gases to report a BrO/Br_y ratio of ~40% compared to a calculated value of ~55% based on kinetics circa 1994. This result contradicts our findings in that Br_y inferred from their BrO would be smaller than Br_y from organics. However, they focused on data collected above 19 km and north of 25°N, where the fractional increase in Br_y due to VSL species is relatively small.

[13] *Pfeilsticker et al.* [2000] found that an additional 3.1 ppt of bromine is needed to reconcile the budget based on balloon-borne profiles of BrO and organic compounds. Their formulation of Br_y^{org} included a contribution of 2.6 ppt from C_nH_mBr_yCl_x compounds. Had they used the WMO definition of Br_y^{org}, their budget discrepancy would have been 5.7 ppt, consistent with our results.

[14] *Simhuber et al.* [2002] and *Schofield et al.* [2004] reported good agreement between column BrO and values found by the SLIMCAT model, for total model Br_y equal to 20 and 21 ppt, respectively, reflecting a 5 to 6 ppt contribution from VSL species. Within SLIMCAT, decomposition of CH₃Br is a surrogate for supply of all stratospheric Br_y. Considering that CH₃Br is shorter lived than halons in the LMS and model Br_y was increased by ~30% relative to WMO Br_y, our results are generally consistent with these two studies. As shown in the auxiliary material¹, the stratospheric vertical column of BrO given by *Schofield et al.* [2004] is consistent with values of Br_y^{TROP} between 4 and 8 ppt when compared to calculations of column BrO from the AER model.

3. Ozone Trends

[15] Figure 4 compares observed trends in column ozone between 35–60°N and 35–60°S to computed trends from the AER 2D model for three scenarios: Br_y^{TROP} of 0, 4, and 8 ppt. No trend is imposed on the Br_y^{TROP}, since presumably the sources are mainly biogenic. Rather, the model is run using the WMO Ab scenario for time evolution of Br_y, Cl_y, CH₄, aerosols, etc, with Br_y then increased by either 4 or 8 ppt at each model level and all times. Although use of a constant Br_y offset is a simplification, it captures the essence of what appears to be occurring. Most of the bromine from VSL gases that cross the tropopause is likely released below 16 km, where the computed effect on ozone trends is largest (Figure 5d). Also, a constant offset is straightforward to implement in global models. Ozone column data, smoothed as described in the report, are from figure 4-33 of *WMO* [2003]. Calculations from the AER model are identical to those presented in chapter 4 of *WMO* [2003] except we use reaction rates from the most recent compendium [*Sander et al.*, 2003]. Use of the latest rate constants reduces the computed ozone depletion by about 13% relative to results presented in *WMO* [2003] (auxiliary material¹).

[16] Enhanced Br_y in the LMS increases computed ozone depletion, particularly during times of elevated aerosol loading due to volcanic activity. The model accounts for ~65% and ~75% of the observed depletion in the 35–60°N and 35–60°S regions, respectively, for Br_y^{TROP}=0. Better overall agreement, ~92% of measured ozone loss in each hemisphere, is achieved for runs using Br_y^{TROP}=8 ppt, a value consistent with the BrO observations presented above. The AER model, like most other models used in the *WMO* [2003] assessment, is less capable of describing year-to-year variations of ozone in the 35–60°S region, which might be due to poor representation within models of ozone-depleted air exported

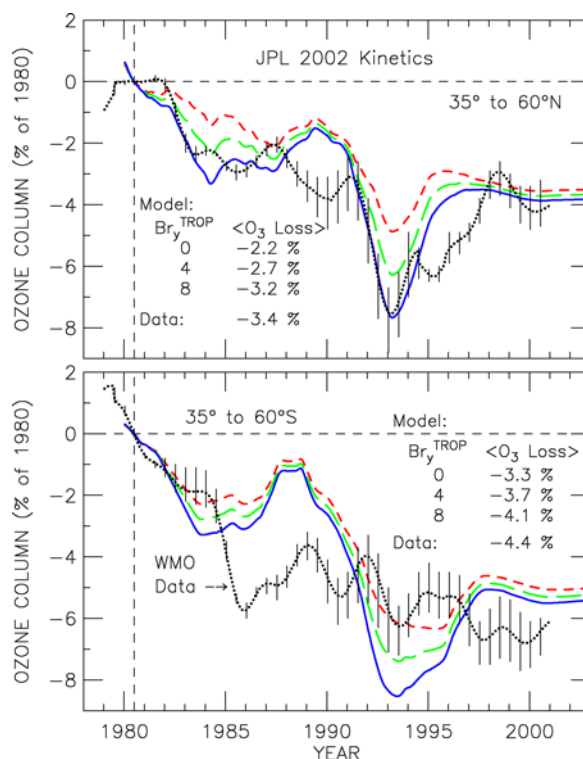


Figure 4. Calculated change in column ozone relative to 1980 levels found using the AER model for Br_y^{TROP} of 0, 4, and 8 ppt (same line types as Fig. 1) for 35–60°N (top) and for 35–60°S (bottom) compared to observed trends in column ozone (black dotted lines) [*WMO*, 2003]. Each panel includes numerical values for the average of the modeled and measured ozone depletion, from the start of 1980 to the end of 2000 (details in auxiliary material¹).

from the vortex or to improper aliasing of the 11-yr solar cycle, the QBO, and volcanic aerosol effects in the smoothing of O₃ column data performed by WMO [R. Stolarski, private communication, 2004]. Regardless, model calculations presented here demonstrate that ozone depletion is increased by the presence of enhanced bromine in the LMS, as suggested by *WMO* [2003] (pg 4.46-4.47).

[17] Figure 5 provides a look into the model photochemistry and O₃ loss. Contributions to O₃ loss by catalytic cycles at 47°N (March 1993) are shown, as well as the change in O₃ profile at 47°N between March 1980 to March 1993. Increased O₃ depletion associated with enhanced bromine is due mainly to a greater role for catalytic loss by the BrO+ClO cycle. Larger BrO concentrations provide a reaction partner for ClO, which in March 1993 was enhanced by increased aerosol following the Mt. Pinatubo eruption. For non-zero Br_y^{TROP}, ozone loss below ~14 km changes from being dominated by pure HO_x photochemistry to a situation where loss by the BrO+HO₂ cycle is considerable. Enhanced loss by the BrO+HO₂ cycle in the LMS occurs for all years of the simulation; this feature is not driven by volcanic aerosol.

[18] Reductions in the O₃ profile revealed by the time slice in Figure 5d peak at 16 km, the altitude where fractional contribution to O₃ loss by the BrO+ClO cycle also maximizes. Observations reveal that loss of O₃ peaked near 16 km over the time period 1980-

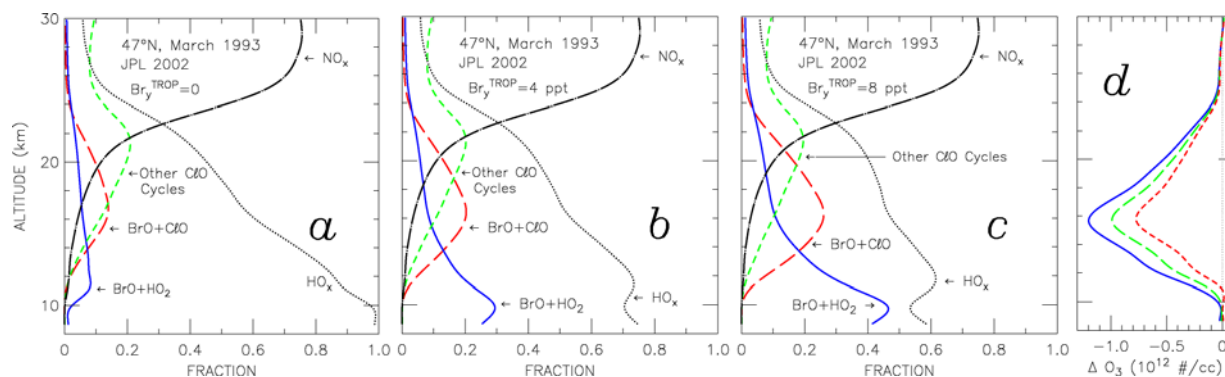


Figure 5. Fraction of odd oxygen loss by various catalytic cycles within the AER model at 47°N, March 1993, for model runs with $\text{Br}_y^{\text{TROP}}$ of 0, 4, and 8 ppt (panels a-c, as indicated). Panel d. Difference between the ozone profile at 47°N, March 1993 and the profile at 47°N, March 1980 for runs with $\text{Br}_y^{\text{TROP}}$ of 0, 4, and 8 ppt (same line types as Figure 1).

1996 [figure 4-13, WMO, 2003]. Calculated trends in O_3 are small at altitudes where loss from the $\text{BrO}+\text{HO}_2$ cycle peaks because we have assumed constant $\text{Br}_y^{\text{TROP}}$.

4. Concluding Remarks

[19] Enhancements to lower stratospheric Br_y are probably due primarily to biogenic gases. Many of these compounds are produced by coastal seaweed populations that might be affected by processes such as El Niño or changes in ocean temperature, circulation, and nutrient supply [Carpenter and Liss, 2000]. The delivery of Br_y to the tropopause depends on the interaction of convective and chemical processes in the upper troposphere [WMO, 2003] that might vary interannually. It is important to quantify the source gases and processes that appear to be responsible for supply of Br_y to the tropopause and to understand possible, associated climate-chemistry interactions [Quack et al., 2004].

[20] Acknowledgments. We thank R. Schofield for helpful discussions and sharing results prior to publication, W. Randel for sharing O_3 trend data files, F. Goutail for providing SAOZ BrO data files, and the reviewers for constructive comments. Research at the Jet Propulsion Laboratory, California Institute of Technology, is performed under contract with the National Aeronautics and Space Administration (NASA). Research at the Smithsonian Astrophysical Observatory is supported by NASA and the Smithsonian Institution. Work at AER is funded by the NASA ACPMAP and SOSST programs.

Notes

1. Supporting material is available via Web browser or anonymous FTP from <ftp://kosmos.agu.org>, directory "apend"; subdirectories in the ftp site are arranged by paper number. Information on electronic supplements is at http://www.agu.org/pubs/esupp_about.html.

References

Avallone, L.M., et al., In situ measurements of BrO during AASE II, *Geophys. Res. Lett.*, 22, 831-834, 1995.
 Carpenter, L.J., and P.S. Liss, On temperate sources of bromoform and other reactive organic bromine gases, *J. Geophys. Res.*, 105, 20539-20547, 2000.
 Chance, K., Analysis of BrO measurements from GOME, *Geophys. Res. Lett.*, 25, 3335-3338, 1998.

Dvortsov, V.L., et al., Rethinking reactive halogen budgets in the lower stratosphere, *Geophys. Res. Lett.*, 26, 1699-1702, 1999.
 Khalil, M.A.K. and R.A. Rasmussen, The trend of CBrClF₂ and other Br-containing gases at the South Pole, *Antarct. J. U.S.*, 19, 206-207, 1985.
 Ko, M.K.W., et al., On the relation between stratospheric chlorine/bromine loading and short-lived tropospheric source gases, *J. Geophys. Res.*, 102, 25507-25517, 1997.
 Pfeilsticker, K., et al., Lower stratospheric bromine budget for the Arctic winter 1998/99, *Geophys. Res. Lett.*, 27, 3305-3308, 2000.
 Platt, U., and G. Hönninger, The role of halogen species in the troposphere, *Chemosphere*, 52, 325-338, 2003.
 Pundt, I., et al., Climatology of stratospheric BrO vertical distribution by balloon-borne UV-visible spectrometry, *J. Geophys. Res.*, 107 (D24), 4806, doi:10.1029/2002JD002230, 2002.
 Pratt, G.C., et al., An assessment of air toxics in Minnesota, *Environ. Health Perspect.*, 108, 815-825, 2000.
 Quack, B., et al., Oceanic CHBr_3 sources for the tropical atmosphere, *Geophys. Res. Lett.*, 31, L23S05, doi:10.1029/2004GL020597, 2004.
 Sander, S.P., et al., JPL 2002: Chemical Kinetics and Photochemical Data for Atmospheric Studies, JPL Pub. 02-25, Jet Propulsion Lab, Pasadena, CA, 2003.
 Schauffler, S.M., et al., Distributions of brominated organic compounds in the troposphere and lower stratosphere, *J. Geophys. Res.*, 104, 21513-21535, 1999.
 Schofield, R., et al., Retrieved tropospheric and stratospheric BrO columns over Lauder, NZ, *J. Geophys. Res.*, 109, D14304, doi:10.1029/2003JD004463, 2004.
 Sinnhuber, B-M., et al., Comparison of measured and modeled stratospheric BrO, *J. Geophys. Res.*, 107(D19), 4398, doi:10.1029/2001JD000940, 2002.
 Sturges, W.T. et al., Bromoform as a source of stratospheric Br_y , *Geophys. Res. Lett.*, 27, 2081-2084, 2000.
 Wamsley, P.R., et al., Distribution of H-1211 in the UT and LS and the 1994 bromine budget, *J. Geophys. Res.*, 103, 1513-1526, 1998.
 WMO, World Meteorological Organization, Global ozone research and monitoring project, Report No. 47, Scientific assessment of ozone depletion: 2002, Geneva, Switzerland, 2003.

R.J. Salawitch, JPL, Mail Stop 183-601, 4800 Oak Grove Drive, Pasadena, CA 91106, USA (rjs@caesar.jpl.nasa.gov)

D. K. Weisenstein, AER, 131 Hartwell Ave., Lexington, Mass. 02421, USA.

L. J. Kovalenko and P.O. Wennberg, GPS, Caltech, Pasadena, CA, 91125, USA.

C.E. Sioris and K. Chance, Harvard-Smithsonian CFA, 60 Garden Street, Mail stop 50, Cambridge, MA, 02138, USA.

M.K.W. Ko, NASA LARC, 21 Langley Blvd, Mail Stop 401 B, Hampton, VA, 23681, USA.

C. McLinden, Met. Ser. Canada, 4905 Dufferin St, Toronto, Ontario M3H 5T4, Canada.

Auxiliary Material for Salawitch et al., Sensitivity of Ozone to Bromine in the Lower Stratosphere, Manuscript 2004GL021504

Quantification of Br_y^{TROP}

The main body of the paper states “the bromine content of the stratosphere is much larger than within the AER model for the WMO Br_y scenario (differences quantified in auxiliary material)”. The purpose of this section of the auxiliary material is to quantify the inorganic bromine offset (i.e., value of Br_y^{TROP}) that, when added to the value of Br_y calculated from the decomposition of long lived organic bromocarbons, agrees best with the data points for “ Br_y from BrO ” shown in Figure 1 (these data points termed Br_y^{BrO} here). We use estimates of Br_y from the decomposition of long-lived organics that are found two ways:

- the relation given in *Wamsley et al.* [1998] based on observations of CH_3Br , Halon-1211, Halon-1301, Halon-2402, CH_2Br_2 , and CH_2BrCl (this relation termed $Br_y^{Org:Wamsley}$)
- the relation calculated using the AER model based on supply of stratospheric bromine from the decomposition of CH_3Br , Halon-1211, Halon-1301, Halon-2402, and Halon-1202 according to the WMO Ab baseline scenario described in table 1-16 of *WMO* [2003] (this relation termed $Br_y^{Org:AER}$).

We first consider the value of Br_y^{TROP} needed to give best agreement between Br_y inferred from BrO (Br_y^{BrO}) and the Wamsley organic bromine relation ($Br_y^{Org:Wamsley}$). For the 87 data points of Br_y^{BrO} versus CFC-11 shown in Figure 1, we have evaluated $Br_y^{Org:Wamsley}$ at the corresponding value of CFC-11, to arrive at the quantity $Br_y^{Org-Fit}$:

$$Br_y^{Org-Fit}(CFC-11) = Br_y^{Org:Wamsley}(CFC-11) + Br_y^{TROP} \quad (1)$$

The mean difference between this $Br_y^{Org-Fit}$ and the data points Br_y^{BrO} is computed:

$$\langle DIFF \rangle = 1/87 \times \sum (Br_y^{BrO} - Br_y^{Org-Fit}) \quad (2)$$

where the summation is carried out for the 87 data points. The resulting difference, as a function of Br_y^{TROP} , is shown in Figure 6a. To minimize the least squares difference of $Br_y^{Org-Fit}$ with respect to the data points for Br_y^{BrO} , we define the cost function:

$$\langle RESID \rangle = \text{sqrt} [1/87 \times \sum (Br_y^{BrO} - Br_y^{Org-Fit})^2] \quad (3)$$

where again the summation is carried out for the 87 data points. The resulting cost function is plotted versus Br_y^{TROP} in Figure 6b. It is evident from Figures 6a and 6b that, in a least squares statistical sense, a value of Br_y^{TROP} equal to 4.2 ppt is most consistent with the values of Br_y^{BrO} reported by *Wamsley et al.* [1998].

The same analysis is repeated using the organic Br_y relation from the AER model for September 1994 at 35°N (i.e., the relations shown in Figure 1b). Here, $Br_y^{Org:AER}$ replaces the quantity $Br_y^{Org:Wamsley}$ in equation (1). Resulting values of $\langle DIFF \rangle$ and $\langle RESID \rangle$ are shown in Figures 6c and 6d. The best fit to the data for Br_y^{BrO} , in a least squares sense, is found for a value of Br_y^{TROP} equal to 6.9 ppt.

The difference between least squares fit values for Br_y^{TROP} of 4.2 ppt (for $Br_y^{Org:Wamsley}$) and 6.9 ppt (for $Br_y^{Org:AER}$) is consistent with our understanding of how these two organic relations were computed. The *Wamsley et al.* [1998] relation includes contributions from CH_3Br , halons, plus CH_2Br_2 and CH_2BrCl . The AER calculation, based on the WMO [2003] scenario, considers contributions to Br_y from only CH_3Br and halons. The contribution of CH_2Br_2 and CH_2BrCl to stratospheric Br_y is about ~2.3 ppt [*Wamsley et al.*, 1998]. These gases decompose quickly in the stratosphere (shorter lifetime than CH_3Br), and hence most of the bromine released from these source molecules is available just above the tropopause (e.g., plate 1 of *Wamsley et al.* [1998]).

The Br_y versus CFC-11 relation from *Wamsley et al.* [1998] shown in Figure 1a exhibits more curvature than the relation from the AER model shown in Figure 1b. The difference of these two relations follows rather closely the shape of the expected contribution to Br_y from CH_2Br_2 and CH_2BrCl , computed from equation (14) of *Wamsley et al.* [1998]. Hence, the difference in the shape of these two Br_y relations is largely due to the shorter stratospheric lifetimes of CH_2Br_2 and CH_2BrCl , relative to the lifetimes of CH_3Br and halons.

Finally, Halon-1202 is considered by *WMO* [2003], but not by *Wamsley et al.* [1998]. The tropospheric abundance of this gas was ~0.05 ppt in the year 2000 [table 1.16, *WMO*, 2003]. The ~0.1 ppt of Br_y associated with Halon-1202 is negligible in the context of our present study, and it is of no consequence to our results that some studies have neglected to consider contributions of this gas to Br_y .

In the main body of the paper, we have chosen to show model results using Br_y^{TROP} values of 0, 4, and 8 ppt rather than using the “best fit” value of 6.9 ppt from the AER relation shown in Figures 1b, 6c and 6d. This choice was made because our intent is to show the sensitivity of ozone loss to bromine, rather than to “overly interpret” the best fit value of Br_y^{TROP} resulting from the analysis of the in situ

data. Indeed, the best fit to the value of Br_y^{BrO} inferred from the *Pundt et al.* [2002] measurements of BrO is for a value of $\text{Br}_y^{\text{TROP}} \geq 8$ ppt (Figure 2).

A possible criticism of our approach could be that the VSL organics require some time to release their bromine, once air masses containing these gases enter the stratosphere. As a result, use of an “offset” to the model Br_y relations is an oversimplification. However, the data for Br_y^{BrO} from observations of BrO shown in Figures 1 and 2 plus the data for BrO vertical column shown in Figure 8 all suggest that the enhanced bromine is released in the lowermost stratosphere, near the 16 km point at mid-latitudes where enhanced bromine has its largest effect on calculated ozone trends. Even though use of a constant offset is somewhat of a simplification, it captures the essence of what appears to be occurring and it is also a straightforward parameterization to implement in any model of global ozone photochemistry. Indeed, it will be interesting to see how other models evaluate the impact on ozone trends and ozone photochemistry of $\text{Br}_y^{\text{TROP}}$ values of 4 and 8 ppt, which we hope our work will motivate. The results will likely depend on the abundance of ClO found in the lowermost stratosphere of the various models, and hence could differ from results shown here given the complexities involved with calculating ClO for this region of the atmosphere (e.g., descent, heterogeneous chemistry, availability of NO_x to sequester ClO and ClONO_2 , etc).

Calculation of Br_y from SAOZ BrO

Figure 2 presents a calculation of Br_y from balloon-borne, spectroscopic SAOZ measurements of BrO obtained at 22°S on November 29, 1997 by *Pundt et al.* [2002]. To our knowledge, this is the only published profile of BrO in the tropics. The purpose of this section is to describe how Br_y was calculated from this profile of BrO.

We have used our photochemical box model [e.g., *Salawitch et al.*, 2002] to estimate Br_y associated with BrO at each altitude. Model inputs are shown in Table 1. Data files were provided by F. Goutail [private communication, 2004]; the profile of BrO is identical to that shown in figures 8, 9, and 11 of *Pundt et al.* [2002]. Model inputs for O_3 , temperature, pressure, and SZA are based on SAOZ measurements and ephemeris. Model inputs for N_2O , CH_4 , and H_2O are from the URAP (UARS Reference Atmospheric Project) model atmosphere, available on-line at: <http://code916.gsfc.nasa.gov/Public/Analysis/UARS/urap/home.html>. We have used the URAP data since no tracers were measured on this SAOZ flight. Input NO_y was estimated from URAP N_2O using the relation of *Popp et al.* [2001]. The profile for stratospheric sulfate aerosol loading is from the SAGE climatology of *Thomason et al.* [1997], updated to include data acquired during November 1997 [L. Thomason, private communication, 2004]. Other quantities input to the model include Cl_y , CO , H_2 , and C_2H_6 . Inputs for these quantities are also based on published observations, but since these parameters have no bearing on the calculated Br_y profile, values are not given in Table 1. The SZAs given in Table 1 are for evening.

Table 1 also contains the total 1σ measurement uncertainty for BrO. Two values are given, reflecting lower and upper bounds. These uncertainties were calculated based on information provided in table 3 and paragraph [34] of *Pundt et al.* [2002]. We have combined measurement accuracy and precision in quadrature to arrive at the total uncertainty. At lower altitudes, the ~1.5 ppt precision for BrO makes the largest contribution to the total uncertainty.

Model results for calculated Br_y are shown in Table 2. The value of Br_y was treated as a free parameter in the box model, and was adjusted until measured and modeled BrO matched for the SZA of observation. A similar Br_y profile is found if values of model inputs for NO_y , H_2O , and CH_4 are taken from the AER 2D model instead of from the URAP model atmosphere.

Two estimates of uncertainty are calculated for model Br_y (Table 2). The first, termed “Meas. Unc.” in Table 2 (thick error bar in Fig. 2), reflects the fractional uncertainty in measured BrO, applied directly to calculated Br_y . The second, termed “Total Unc.” in Table 2 (thin error bar in Fig. 2) represents a RSS combination of “Meas. Unc.” for Br_y with the uncertainty in Br_y due to the kinetic factors that regulate the BrO/ Br_y ratio (“Kin. Unc.”). For the altitudes considered here, BrONO_2 is the dominant unobserved Br_y species. We derived “Kin. Unc.” by carrying out numerous calculations of Br_y , varying the rates of formation and loss of BrONO_2 for the range of uncertainties given by *Sander et al.* [2003]. In all cases, values given in Table 2 represent lower and upper limits for Br_y (or BrO) considering the stated uncertainties.

Figure 2 indicates that Br_y inferred from measured BrO is considerably larger than the estimated value of stratospheric Br_y based solely on supply from CH_3Br +halons. This result is not surprising given that the measured profile of BrO peaks at 15.7 ppt (Table 1), nearly equal to the total bromine content supplied by CH_3Br and halons [*WMO*, 2003]. Peak stratospheric BrO mixing ratios between 15 and 20 ppt are measured on all SAOZ flights (e.g., figure 8 of *Pundt et al.* [2002]). Even though our analysis has focused on the tropical SAOZ flight, it appears that data collected during most (if not all) of the SAOZ flights supports the view that CH_3Br and halons fall far short of supplying the full burden of stratospheric Br_y .

Column BrO from GOME

The main body of the paper states “the vertical column of BrO from GOME [*Chance*, 1998] during May 1997 far exceeds vertical BrO columns from the AER model”. Also, in the main body of the paper, results for the vertical column of BrO from GOME are compared to columns from the AER model, where we have adjusted the GOME data to account for a possible, ubiquitous, global tropospheric mixing ratio of BrO equal to 1 ppt. We also have noted in the paper that the region marked “Enhanced Tropospheric BrO” in Figure 3 would be discussed. Here we present supporting details and discussion of these points, as well as brief background information regarding GOME.

The Global Ozone Monitoring Experiment (GOME) was launched on the European Space Agency (ESA) ERS-2 satellite on April 21, 1995. The satellite is in a sun synchronous polar orbit with a 10:30 am equator crossing time in the descending node. The GOME instrument measures back-scattered radiances over the spectral range 240 to 800 nm. Spectral fits to data acquired between 344 and 360 nm are used to obtain the slant column density of BrO (SCD_{BrO}) [e.g., *Chance*, 1998].

Chance [1998] reported a vertical column density for BrO (VCD_{BrO}) using an air mass factor (AMF) based on the assumption that all of the BrO molecules in the line-of-sight were in the stratosphere:

$$VCD_{BrO} = SCD_{BrO} / AMF_{STRAT} \quad . \quad (4)$$

Radiative transfer calculations show that for solar zenith angles less than 70° , AMF_{STRAT} , the ratio of the path of sunlight through the atmosphere to the vertical path, assuming the absorbing species is present entirely in the stratosphere, is nearly equal to the geometric approximation:

$$AMF_{STRAT} \approx 1/\cos(SZA) + 1/\cos(AAO) \quad , \quad (5)$$

where SZA is solar zenith angle and AAO is the average angle of observation [e.g., *Wagner et al.*, 2001]. For the nadir observations used here, equation (5) reduces to:

$$AMF_{STRAT} \approx 1/\cos(SZA) + 1 \quad . \quad (6)$$

Measurements of VCD_{BrO} from GOME orbit #70502164 on May 2, 1997, assuming all of the absorption is due to stratospheric BrO, are shown in Figure 7a. Error bars, based on the residual of the spectral fits, are shown for every 50th point for clarity. Data are shown for spectra acquired with $SZA < 70^\circ$, to assure the validity of equation (5) for AMF_{STRAT} . These data are very similar to those shown in Figure 5 of *Chance* [1998] except they have been retrieved using the BrO absorption cross section measurements of *Wilmouth et al.* [1999].

Also shown in Figure 7a are estimates of total column BrO from the AER model for April 15, 1997, at local noon, for model runs using values of Br_y^{TROP} equal to 0, 4, and 8 ppt. We have assumed no contribution from the troposphere for model values of BrO column shown here, and in the main body of the paper. Column BrO from the AER model has been determined from the integral of the model BrO profile above the chemical tropopause, defined as the pressure for which the abundance of ozone first reaches a value of 0.1 ppm.

Figure 7a shows that, if the BrO column observed by GOME is assumed to reside entirely in the stratosphere, the abundance of VCD_{BrO} measured by GOME is much larger than the amount of stratospheric BrO found for any of the AER model runs. All data in Figure 7 are restricted to $SZA < 70^\circ$. Even though the model results are for local noon and the GOME estimates of VCD_{BrO} are for various times of day (close to 10:30 am local time, except near the poles), off-line photochemical model calculations demonstrate that no significant part of the difference between measured and modeled BrO can be explained by diurnal variations in the BrO column, which varies slowly during the sunlit portion of the day according to known chemistry.

We have also computed the residual *stratospheric* column of BrO from GOME, termed $VCD_{BrO-STRAT}$, assuming that a portion of the BrO signal observed by GOME is due to BrO molecules residing in the troposphere. We use the formulation:

$$VCD_{BrO-STRAT} = [SCD_{BrO} - AMF_{TROP} \times VCD_{BrO-TROP}] / AMF_{STRAT} \quad , \quad (7)$$

where SCD_{BrO} is the slant column density of BrO [same quantity as in equation (4)], $VCD_{BrO-TROP}$ is the hypothetical column density of BrO below the tropopause, and AMF_{TROP} is the ratio of the path of sunlight through the atmosphere to the vertical path assuming the absorbing species is in the troposphere. Radiative transfer calculations show that AMF_{TROP} typically cannot be described by a simple geometric approximation [e.g., section 2 of *Wagner et al.*, 2001]. Our estimates of AMF_{TROP} are based on radiative transfer calculations similar to those described by *Zeng et al.* [2003]. The value of AMF_{TROP} can differ substantially from AMF_{STRAT} , particularly for SZA larger than $\sim 60^\circ$ [e.g., figure 1 of *Wagner et al.*, 2001], due to differences in the penetration and extinction of incoming solar radiation. Also, AMF_{TROP} is sensitive to ground albedo, which is not the case for AMF_{STRAT} [*Wagner et al.*, 2001]. We have used the actual albedo of each GOME pixel for our calculation of AMF_{TROP} as well as tropopause height (as a function of latitude) based on the chemical tropopause from the AER model for April 15, 1997.

We have not accounted for the possible presence of clouds in the analysis presented here. Clouds can shield from the view of GOME absorbing species located below cloud top and must be considered when quantifying the contribution of boundary layer BrO to the GOME measurement of SCD_{BrO} [*Wagner et al.*, 2001]. Interestingly, for GOME measurements of BrO acquired over the mid-Pacific Ocean in October 1997 (e.g., observations far removed from local Arctic sources of halogens), there appears to be no significant correlation between column BrO and cloud cover [*Chance et al.*, 1998]. This result suggests the majority of any possible tropospheric absorption is occurring above the cloud tops (e.g., in the free troposphere). The value of $VCD_{BrO-TROP}$ used in equation (7) was found by assuming a uniform BrO mixing ratio throughout

the troposphere, with tropopause height based on the chemical tropopause from the AER model (e.g., variable tropopause height versus latitude). Assuming that 1 ppt of BrO is uniformly distributed throughout the troposphere, the difference between VCD_{BrO} and $VCD_{BrO-STRAT}$ varies from $\sim 2.0 \times 10^{13}$ molecules/cm² at 35°S and the equator, to $\sim 2.2 \times 10^{13}$ molecules/cm² at 35°N, and rises to $\sim 3.0 \times 10^{13}$ molecules/cm² at 60°N.

Figures 7b-e show comparisons of $VCD_{BrO-STRAT}$ to the stratospheric column of BrO from the AER model, for values of tropospheric BrO mixing ratio of 0.5 ppt, 1 ppt, 1.5 ppt, and 2 ppt, respectively. Note the shift in the y-axis of Figures 7d and 7e, relative to the other panels, to show data points that drop below zero when larger tropospheric contributions are subtracted from the GOME BrO signal.

The region marked “enhanced tropospheric BrO” corresponds to observations over Hudson Bay, which show large increases in column BrO on May 2, 1997 due to release of bromine from the snow and ice pack [Chance, 1998; Zeng et al., 2003]. Aircraft observations obtained during April 26, 1997 show that enhanced BrO exists throughout the high-latitude, free troposphere (e.g., above the planetary boundary layer) [McElroy et al., 1999]. We have not made any attempt to increase $VCD_{BrO-TROP}$ for data collected in this region. Rather, our goal is to examine how the overall comparison between measured and modeled BrO columns shown in Figure 7a evolves if we assume a portion of the GOME signal is due to varying amounts of a possible, ubiquitous, tropospheric abundance of BrO.

The comparison in Figure 7c shows that, even for a background level of tropospheric BrO of 1 ppt, the contribution of stratospheric BrO to the GOME signal exceeds stratospheric column BrO from the AER model for the WMO [2003] Br_y scenario. Reasonable agreement (e.g., overlap of error bars at most latitudes, except for the region marked “enhanced tropospheric BrO”) is achieved for the AER model run using Br_y^{TROP} = 8 ppt. The quantity Br_y^{TROP} refers to Br_y released from all sources for air that has ascended to the *tropopause*, which is not to be confused with the ubiquitous background level of tropospheric BrO that might be present at all altitudes. Of course, global background tropospheric BrO would likely contribute to Br_y^{TROP}. For a tropospheric BrO of 2 ppt (Figure 7e), $VCD_{BrO-STRAT}$ exhibits closer overall agreement with stratospheric column BrO from the AER model. However, the latitudinal structure of modeled and measured BrO columns are not in very good agreement for this case.

The comparisons shown in Figure 7 are meant to motivate the need to achieve a consistent picture of the *atmospheric* distribution of BrO. It is likely that the large discrepancy between GOME VCD_{BrO} and column BrO found within many models (e.g., Figure 7a) is caused by a combination of contributions from both the *troposphere* and the *stratosphere* that are not properly represented in these models. It is probably too simple to ascribe the entire difference between GOME VCD_{BrO} and column BrO from the AER model, for the WMO Br_y scenario, to tropospheric BrO. Many attempts have been made to define the global background tropospheric abundance of BrO, from both ground-based and space-based techniques that use a variety of assumptions. A comprehensive review is beyond the scope of our paper or this auxiliary material section, but a summary is given in section 6 of Platt and Hönniger [2003]. These methods typically find values for average tropospheric BrO ranging from 1 to 2 ppt [Platt and Hönniger, 2003]. However, a recent study of ground-based diffuse and direct sunlight over Lauder, NZ (45°S) suggests a mean value for tropospheric BrO of only 0.2 ppt, and an upper limit of 0.9 ppt [Schofield et al., 2004]. Clearly, more work remains to define the cause of the imbalance between modeled and measured total column BrO. The results in Figure 3 of our paper, and in Figure 8 of the auxiliary material, suggest a consistent picture with many observations might be achieved for a tropospheric background level of ~ 1 ppt and enhancements in stratospheric Br_y, relative to the WMO Br_y scenario, ranging from 4 to 8 ppt.

Column BrO from Ground-Based Measurements

The main body of our paper states “the stratospheric vertical column of BrO given by Schofield et al. [2004] is consistent with values of Br_y^{TROP} between 4 and 8 ppt when compared to calculations of column BrO from the AER model”. The purpose of this section is to illustrate these comparisons and to comment further on ground-based measurements of column BrO.

Proper interpretation of the stratospheric implications of column BrO is challenged by the need to distinguish the stratospheric and tropospheric contributions to the measurement. Schofield et al. [2004] examined diffuse and direct sunlight, at solar zenith angles of 80°, 84°, and 87°, to quantify contributions to the total column from the stratosphere and troposphere. As discussed in the main body of our paper, they reported good agreement between the retrieved stratospheric column BrO and values found using the SLIMCAT model, for total model Br_y of 21 ppt. This level of Br_y represents a contribution of 6 ppt to the stratospheric budget from VSL organic bromine source gases [Schofield et al., 2004].

Figure 8 compares the Schofield et al. [2004] measurement of stratospheric BrO to values found using the AER model. In this comparison, model results for BrO at noon are shown, since this quantity is routinely saved during long-term ozone loss simulations. The measured BrO column of $2.35 \pm 0.47 \times 10^{13}$ molecules/cm² found for SZA=80° is shown, along with a data point scaled to noon, $2.80 \pm 0.56 \times 10^{13}$ molecules/cm². Model curves shown in figure 8 of Schofield et al. [2004] were used to estimate the change in BrO column between SZA=80° and noon; similar scaling factors are found using our photochemical model.

Calculations of column BrO at noon from the AER model, found for March 2003, are shown for model runs using Br_y^{TROP} of 0, 4, and 8 ppt. The measurement of Schofield et al. [2004], scaled to noon, is most consistent with a value for

$\text{Br}_y^{\text{TROP}}$ of ~6 ppt. This comparison is shown to support the statement in the paper that our finding of a significant offset to the Br_y vs tracer curve, of magnitude between 4 and 8 ppt, is “generally consistent with the findings of *Schofield et al.* [2004]”.

We conclude this section by noting that direct comparison of BrO from the AER model to ground-based BrO column measurements reported by *Sinnhuber et al.* [2002] is beyond the scope of this paper. *Sinnhuber et al.* [2002] focused on “Differential Slant Column Density” (DSCD) of BrO. Computation of DSCD BrO requires tying global model calculations of BrO profiles to a multiple scattering radiative transfer code that is accurate for twilight conditions. *Sinnhuber et al.* [2002] reported “the absolute amount of the BrO slant columns is consistent with a total stratospheric bromine loading of 20 ± 4 ppt for the period 1998-2000”. This abundance represents a ~5 ppt contribution from VSL species. In their study, CH_3Br was used as a surrogate for the stratospheric entry of all bromine compounds (e.g., the calculated Br_y vs tracer relation did not explicitly account for the shorter lifetimes of VSL species).

Considering the various uncertainties of the *Sinnhuber et al.* [2002] study, it appears their measurements might be consistent with our view of non-zero Br_y near the tropopause. For most of the stations that measured BrO, they reported that observed DSCD exceeds modeled DSCD (found using $\text{Br}_y=20$ ppt) by about 10% (paragraph [28]). Furthermore, potential contributions to calculated DSCD BrO due to aerosol scattering and tropospheric BrO were not considered in the base case of *Sinnhuber et al.* [2002]. Both of these factors, examined in table 3 of their paper, would lead to an inference of higher levels of stratospheric Br_y . It would be interesting to see comparisons of measured and modeled DSCD BrO, following a treatment for the stratospheric entry of Br_y in a 3D model similar to that outlined in the main body of our paper.

The Effect of JPL 2002 Kinetics on Ozone Trends, The Statistics of Measured and Modeled Ozone Trends, and Additional Comments on Ozone Trends

The main body of the paper states “use of the latest rate constants [within the AER 2D model] reduces the computed ozone depletion relative to results presented in *WMO* [2003] by about 13% (auxiliary material)”. Also, numerical values for measured and modeled ozone loss are given in Figure 4 and discussed in the text. Supporting details are described here.

As noted in the main body of the paper, most 2D and 3D ozone assessment models fail to account for the full extent of observed depletion of column ozone at Northern Hemisphere mid-latitudes when using scenarios for the time evolution of Cl_y , Br_y , CH_4 , N_2O , and aerosol loading prescribed by *WMO* [2003] [e.g., Figure 4 of our paper; figure 4-33 of *WMO*, 2003; see also *Solomon et al.*, 1994; *Jackman et al.*, 1996; and *Solomon et al.*, 1997]. Models compare more favorably to observations of total ozone depletion between 60°S and 60°N, but this comparison hides problems such as the fact that most models find considerable ozone loss in the tropics, a region where little loss is actually observed [*WMO*, 2003; *Andersen et al.*, 2004]. Models also fail to capture the vertical profile of ozone loss, particularly below 20 km altitude [figure 4-30, *WMO*, 2003].

Details of the implementation of the AER model used here and in *WMO* [2003] are given by *Rinsland et al.* [2003]. For these calculations, year-to-year temperature variability was included in the model between 1979 and 1995. Climatological temperatures were used for following years. Climatological transport parameters were used for all years of the simulation.

The comparison between modeled and measured ozone depletion shown in *WMO* [2003] will get worse once models adopt the latest kinetics formulation [*Sander et al.*, 2003; hereafter JPL 2002]. Presently, published studies of ozone depletion rely on JPL 2000 kinetics [*Sander et al.*, 2000]. Figure 9 shows a comparison of calculated changes in ozone, between 35°–60°N and between 35°–60°S, for runs of the AER model with $\text{Br}_y^{\text{TROP}}$ set to zero, using JPL 2000 kinetics and using rate constants from JPL 2002. Both the data and the AER model results using JPL 2000 kinetics shown in Figure 9 are exactly the same as shown in figure 4-33 of *WMO* [2003]. We expect that the amount of ozone depletion found by most ozone assessment models will become smaller relative to the values found in *WMO* [2003], by an amount comparable to that shown in Figure 9, once the latest rate constants are adopted.

The most significant change between JPL 2000 and JPL 2002 is the almost factor of 2 reduction in the rate constant for $\text{ClO}+\text{HO}_2\rightarrow\text{HOCl}+\text{O}_2$. This accounts for about 2/3 of the difference between the JPL 2000 and JPL 2002 curves shown in Figure 9. The rest of the difference is due mainly to the JPL 2002 update for the rate constant of $\text{OH}+\text{NO}_2+\text{M}\rightarrow\text{HNO}_3+\text{M}$. There are research issues associated with both of these rate constants, such as: Why do large differences persist in laboratory measurements of the $\text{ClO}+\text{HO}_2$ rate constant reported by various groups? Can atmospheric measurements of HOCl be used to shed light on the rate of stratospheric ozone loss by the $\text{ClO}+\text{HO}_2$ cycle? Does formation of stable HOONO by the reaction $\text{OH}+\text{NO}_2+\text{M}$ preclude use of a simple Troe expression for the rate constant?

We note also that if the amount of bromine in the lowermost stratosphere represented by model runs with $\text{Br}_y^{\text{TROP}}$ of 4 or 8 ppt is realistic, then the catalytic cycle limited by the $\text{BrO}+\text{HO}_2$ reaction has increased importance for photochemical loss of ozone in this region (Figure 5). This catalytic cycle might also be responsible for significant loss of ozone in the free troposphere [*von Glasow et al.*, 2004]. In our model simulations, we have assumed that $\text{Br}_y^{\text{TROP}}$ is constant over time. Even though the ozone photochemical lifetime is large below 14 km, variability in $\text{Br}_y^{\text{TROP}}$ might have consequences for past or future changes in column ozone [*Solomon et al.*, 1994]. The $\text{BrO}+\text{HO}_2$ rate constant, which underwent a major revision between the JPL 1994 and JPL 1997 recommendations, is currently uncertain by nearly a factor of 2 at 220 K [*Sander et al.*, 2003]. This reaction likely requires additional laboratory study, particularly at cold temperatures characteristic of the lower stratosphere. Also, the impact of cold-sulfate or sub-visible cirrus on O_3 depletion in the LMS might require a re-evaluation

because BrO associated with *enhanced* Br_y provides a reaction partner for activated ClO, which is an ozone loss process that is not represented in present model evaluations [e.g., *Bregman et al.*, 2002; *WMO*, 2003].

The average values of computed ozone depletion for various runs of the AER 2D model are given in Table 3. Results are shown for the spatial regions 35°–60°N and 35°–60°S, for 6 runs: Br_y^{TROP} values of 0, 4, and 8 ppt, for both JPL 2000 and JPL 2002 kinetics. The quantities in Table 3 represent the average amount of ozone depletion for each model run, from the start of 1980 until the end of 2000 (this time interval is chosen to match availability of data for the ozone time series from *WMO* [2003]). Units are percent per year deviation of column ozone, from the average value of column ozone for the year 1980. Values for the JPL 2002 model runs are also given in Figure 4.

The entries in Table 3 show that the use of JPL 2002 rate constants has the largest effect on computed trends for the northern hemisphere (NH), in the Br_y^{TROP} = 0 ppt model run. This result is due to the ClO+HO₂ cycle having a larger effect on ozone loss, relative to the other loss cycles that involve ClO, for the 35°–60°N region of the model simulation that uses the *WMO* Br_y scenario. For the 35°–60°S region, the ClO+ClO and BrO+ClO cycles are responsible for larger amounts of ozone depletion due to export of air from the simulated ozone hole. As Br_y^{TROP} is increased, all model results are less sensitive to the choice of JPL 2000 versus JPL 2002 kinetics, since the BrO+ClO cycle, which has the same rate constant in both evaluations, has a larger role in the resulting ozone loss. The percentage difference between the ozone depletion from the JPL 2000 and JPL 2002 model runs given in Table 3 has been averaged, using depletion from JPL 2000 in the denominator, to arrive at the value of 13% for the effect of updated kinetics on ozone loss that is given in the main body of the paper.

Table 3 also contains an entry for measured ozone depletion, for the 35°–60°N and 35°–60°S regions, resulting from averaging the data points from *WMO* [2003] shown in Figures 4 and 9, for the time interval from the start of 1980 to the end of 2000 (last time point covered by the *WMO* [2003] data set). Units are percent deviation from the average for the year 1980: e.g., same units as used for the model results in Table 3. These numerical values are also given in Figure 4. The data and the method of smoothing are described in detail by *WMO* [2003]. Results shown here and in *WMO* [2003] are based on a “merged satellite data record” that originates from the work of *Fioletov et al.* [2002].

Comparison of the measured and modeled ozone depletion values in Table 3 is perhaps simplistic, overlooking details such as timing of the ozone loss and response to forcings such as enhanced volcanic aerosols. Nonetheless, the entries reveal that model runs using Br_y^{TROP} = 8 ppt and JPL 2002 rate constants account for ~92% of the overall measured ozone loss between 35°–60°N and for ~93% of the loss between 35°–60°S. In contrast, the JPL 2002 model run using the *WMO* Br_y scenario accounts for ~65% and ~75% of the observed ozone loss in the 35°–60°N and 35°–60°S regions, respectively. This analysis supports the statement in our abstract that “including this additional bromine in an ozone trend simulation increases the computed ozone depletion over the past ~25 years, leading to better agreement between measured and modeled ozone trends.”

References for Auxiliary Material

- Andersen, S. B., E.C. Weatherhead, J. Austin, C. Brühl, E.L. Fleming, J. de Grandpre, V. Grewe, I. Isaksen, G. Pitari, R.W. Portmann, B. Rognerud, J.E. Rosenfield, D. Shindell, S. Smyshlayev, T. Nagashima, G. Velders, D.K. Weisenstein, J. Xia, Comparison of modeled and observed stratospheric ozone springtime maxima, in *Quadrennial Ozone Symposium*, edited by C.S. Zerefos, pp. 155, University of Athens, Kos, Greece, 2004.
- Bregman, B., P.-H. Wang, and J. Lelieveld, Chemical ozone loss in the tropopause region on subvisible ice clouds, calculated with a chemistry-transport model, *J. Geophys. Res.*, 107 (D3), doi:10.1029/2001JD000761, 2002.
- Chance, K., Analysis of BrO measurements from the Global Ozone Monitoring Experiment, *Geophys. Res. Lett.* 25, 3335-3338, 1998.
- Chance, K., R.J.D. Spurr, and T.P. Kurosu, Atmospheric trace gas measurements from the European Space Agency’s Global Ozone Monitoring Experiment, SPIE, Vol. 3495, pg 230-234, Satellite Remote Sensing of Clouds and the Atmosphere III; Jacqueline E. Russell, Ed., Dec., 1998.
- Fioletov, V.E., G.E. Bodeker, A.J. Miller, R.D. McPeters, and R. Stolarski, Global and zonal total ozone variations estimated from ground-based and satellite measurements: 1964-2000, *J. Geophys. Res.*, 107(D22), 4647, doi:10.1029/2001JD001350, 2002.
- Jackman, C.H., E.L. Fleming, S. Chandra, D.B. Considine, and J.E. Rosenfield, Past, present, and future modeled ozone trends with comparisons to observed trends, *J. Geophys. Res.*, 101, 28753-28767, 1996.
- McElroy, C.T., C.A. McLinden, J.C. McConnell, Evidence for bromine monoxide in the free troposphere during the Arctic polar sunrise, *Nature*, 397, 338-341, 1999.
- Platt, U., and G. Hönninger, The role of halogen species in the troposphere, *Chemosphere* 52, 325-338, 2003.
- Popp, P.J., M.J. Northway, J.C. Holecek, R.S. Gao, D.W. Fahey, J.W. Elkins, D.F. Hurst, P.A. Romashkin, G.C. Toon, B. Sen, S.M. Schauffler, R.J. Salawitch, C.R. Webster, R.L. Herman, H. Jost, T.P. Bui, P.A. Newman, and L.R. Lait, Severe and extensive denitrification in the 1999-2000 Arctic winter stratosphere, *Geophys. Res. Lett.*, 28, 2875-2878, 2001.
- Pundt, I., J.-P. Pomereau, M.P. Chipperfield, V. van Roozendaal, and F. Goutail, Climatology of stratospheric BrO vertical distribution by balloon-borne UV-visible spectrometry, *J. Geophys. Res.*, 107 (D24), 4806, doi:10.1029/2002JD002230, 2002.
- Rinsland, C.P., D.K. Weisenstein, M.K.W. Ko, C.J. Scott, L.S. Chiou, E. Mahieu, R. Zander, and P. Demoulin, Post-Mount

- Pinatubo eruption ground-based infrared stratospheric column measurements of HNO₃, NO, and NO₂ and their comparison with model calculations, *J. Geophys. Res.*, *108*, 4437, doi:10.1029/2002JD002965, 2003.
- Salawitch, R.J., P.O. Wennberg, G.C. Toon, B. Sen, and J.-F. Blavier, Near IR photolysis of HO₂NO₂: implications for HO_x, *Geophys. Res. Lett.*, *29*, doi:10.1029/2002GL015006, 2002.
- Sander, S.P., R.R. Friedl, W.B. DeMore, D.M. Golden, M.J. Kurylo, R. F. Hampson, R.E. Huie, G.K. Moortgat, A.R. Ravishankara, C.E. Kolb, M.J. Molina, Chemical Kinetics and Photochemical Data for Use in Stratospheric Modeling, Evaluation No. 13, JPL Publication 00-3, Jet Propulsion Lab, Pasadena, CA, 2000.
- Sander, S.P., R.R. Friedl, D.M. Golden, M.J. Kurylo, R.E. Huie, V.L. Orkin, G.K. Moortgat, A.R. Ravishankara, C.E. Kolb, M.J. Molina, and B.J. Finlayson-Pitts, Chemical Kinetics and Photochemical Data for Use in Atmospheric Studies, Evaluation No. 14, JPL Publication 02-25, Jet Propulsion Lab, Pasadena, CA, 2003.
- Schofield, R., K. Kreher, B.J. Connor, P.V. Johnston, A. Thomas, D. Shooter, M.P. Chipperfield, C.D. Rodgers, and G.H. Mount, Retrieved tropospheric and stratospheric BrO columns over Lauder, New Zealand, *J. Geophys. Res.*, *109*, D14304 doi:10.1029/2003JD004463, 2004.
- Sinnhuber, B.-M., D.W. Arlander, H. Bovensmann, J.P. Burrows, M.P. Chipperfield, C.-F. Enell, U. Frieß, F. Hendrick, P.V. Johnston, R.L. Jones, K. Kreher, N. Mohamed-Tahrin, R. Müller, K. Pfeilsticker, U. Platt, J.-P. Pommereau, I. Pundt, A. Richter, A. M. South, K.K. Tørnkvist, M. Van Roozenfael, T. Wagner, and F. Wittrock, Comparison of measured and modeled stratospheric BrO, *J. Geophys. Res.*, *107*(D19), 4398, doi:10.1029/2001JD000940, 2002.
- Solomon, S., R.R. Garcia, and A.R. Ravishankara, On the role of iodine in ozone depletion, *J. Geophys. Res.*, *99*, 20491-20499, 1994.
- Solomon, S., S. Borrmann, R.R. Garcia, R. Portmann, L. Thomason, L.R. Poole, D. Winker, and M.P. McCormick, Heterogeneous chlorine chemistry in the tropopause region, *J. Geophys. Res.*, *102*, 21411-21429, 1997.
- Thomason, L.W., L.R. Poole, and T. Deshler, A global climatology of stratospheric aerosol surface area density deduced from Stratospheric Aerosol and Gas Experiment II measurements: 1984-1994, *J. Geophys. Res.*, *102*, 8967-8976, 1997.
- Von Glasow, R., R. von Kuhlmann, M.G. Lawrence, U. Platt, and P.J. Crutzen, Impact of reactive bromine chemistry in the troposphere, *Atmos. Chem. Phys. Discuss.*, *4*, 4877-4913, 2004.
- Wagner, T., C. Leue, M. Wenig, K. Pfeilsticker, and U. Platt, Spatial and temporal distribution of enhanced boundary layer BrO concentrations measured by the GOME instrument aboard ERS-2, *J. Geophys. Res.*, *106*, 24225-24235, 2001.
- Wamsley, P.R., J.W. Elkins, D.W. Fahey, G.S. Dutton, C.M. Volk, R.C. Meyers, S.A. Montzka, J.H. Butler, A.D. Clarke, P.J. Fraser, L.P. Steele, M.P. Lucarelli, E.L. Atlas, S.M. Schauffler, D.R. Blake, F.S. Rowland, W.T. Sturges, J.M. Lee, S.A. Penkett, A. Engel, R.M. Stimpfle, K.R. Chan, D.K. Weisenstein, M.K.W. Ko, and R.J. Salawitch, Distribution of halon-1211 in the upper troposphere and lower stratosphere and the 1994 total bromine budget, *J. Geophys. Res.*, *103*, 1513-1526, 1998.
- Wilmouth, D.M., T.F. Hanisco, N.M. Donahue, and J.G. Anderson, Fourier transform ultraviolet spectroscopy of the A ²Π_{3/2} ← X ²Π_{3/2} transition of BrO, *J. Phys. Chem. A.*, *103*, 8935-8945, 1999.
- WMO, World Meteorological Organization, Global ozone research and monitoring project, Report No. 47, Scientific assessment of ozone depletion: 2002, Geneva, Switzerland, 2003.
- Zeng, T., Y. Wang, K. Chance, E.V. Browell, B.A. Ridley, and E.L. Atlas, Widespread persistent near-surface ozone depletion at northern high latitudes in spring, *Geophys. Res. Lett.*, *30*(24), 2298, doi:10.1029/2003GL018587, 2003.

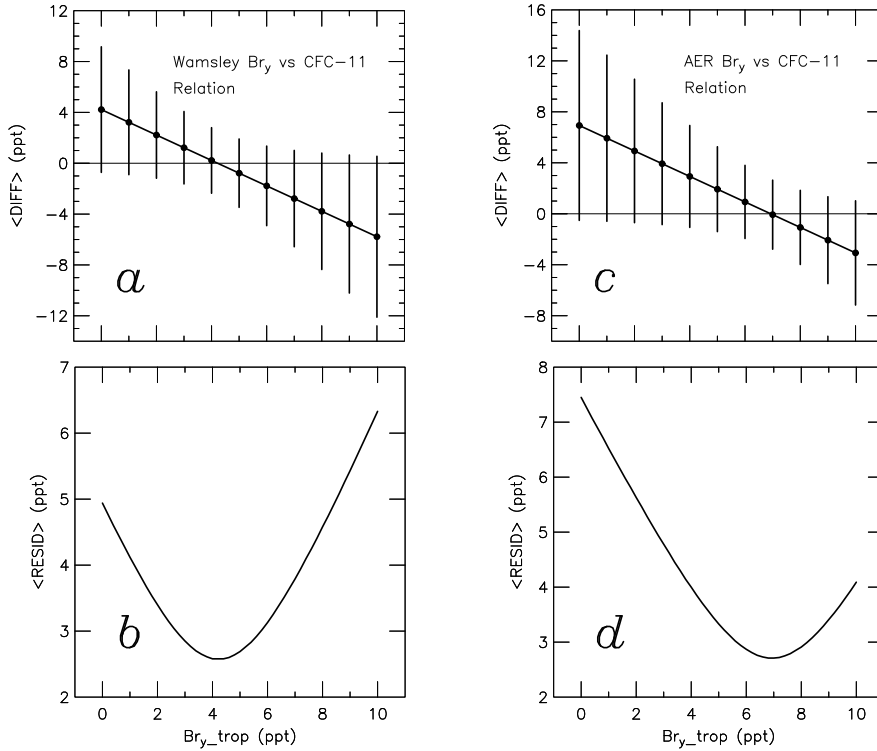


Figure 6. Panel *a*. Mean difference (i.e., $\langle \text{DIFF} \rangle$ in equation (2) of text) between values of Br_y^{BrO} (data points, Figure 1) and values of $\text{Br}_y^{\text{Org-Fit}}$ based on the decomposition of organic bromocarbons given by *Wamsley et al.* [1998] with an additive offset $\text{Br}_y^{\text{TROP}}$, plotted versus $\text{Br}_y^{\text{TROP}}$. Error bars, shown only at integer values of $\text{Br}_y^{\text{TROP}}$ for clarity, are the square root of the mean of the squared residuals (same quantity shown in next panel; see text).

Panel *b* The square root of the mean of the squared residuals ($\langle \text{RESID} \rangle$ in equation (3) of text), as a function of $\text{Br}_y^{\text{TROP}}$. Best fit to the data is for $\text{Br}_y^{\text{TROP}} = 4.2$ ppt.

Panel *c*. Same as panel *a*, except for the Br_y versus CFC-11 relation from the AER model (35°N , September 1994) found using the *WMO* [2003] Br_y baseline scenario Ab.

Panel *d*. Same as panel *b*, except for the AER Br_y versus CFC-11 relation. Best fit is for $\text{Br}_y^{\text{TROP}} = 6.9$ ppt.

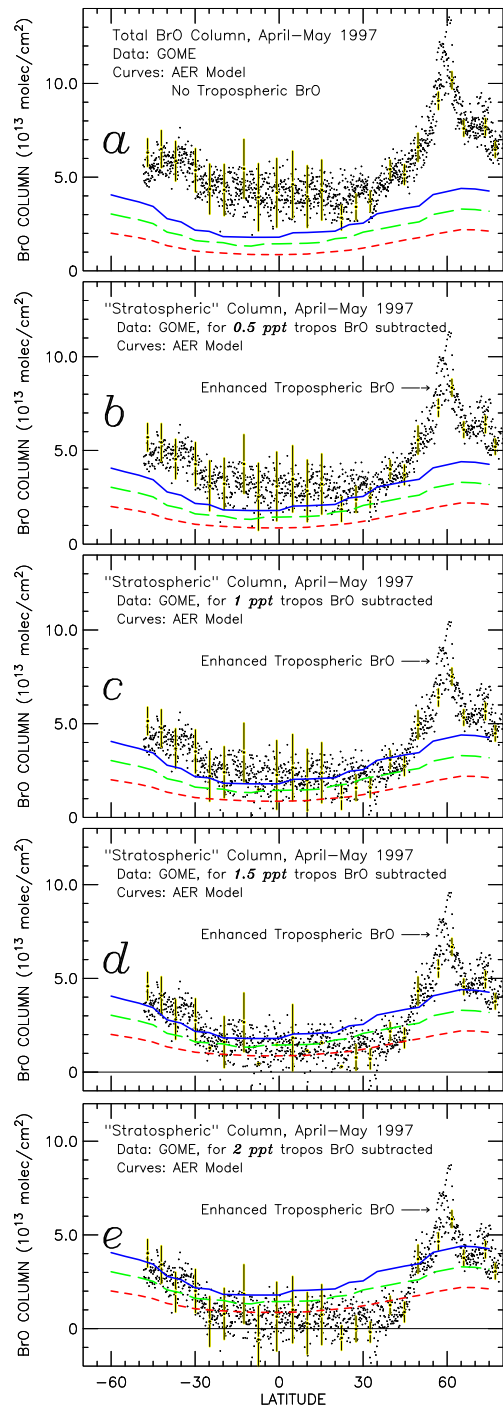


Figure 7. Panel *a*. Total column BrO (late morning) measured by GOME on April 30, 1997 assuming a stratospheric airmass factor (e.g., that all of the BrO was present in the stratosphere) compared to columns above the chemical tropopause from the AER model for April 15, 1997 (local noon), for $\text{Br}_y^{\text{TROP}}$ values of 0 (red short-dashed), 4 (green long-dashed), and 8 (blue solid) ppt. Error bars denote 1σ total measurement uncertainty based on considerations such as residuals in spectral fit as described by *Chance* [1998], and are shown only for every 50th point for clarity. Panels *b* to *e*. The contribution to the GOME signal from BrO in the stratosphere, found by assuming mixing ratios of BrO distributed uniformly in the troposphere (see text for details), at levels of 0.5, 1.0, 1.5, and 2.0 ppt, respectively. Model calculations of stratospheric BrO are the same for all panels. Data acquired over Hudson Bay are noted by "enhanced tropospheric BrO" (see text). The shift in the y-axis for panels *d* and *e* is designed to show data points that fall below zero when larger amounts of tropospheric BrO are subtracted.

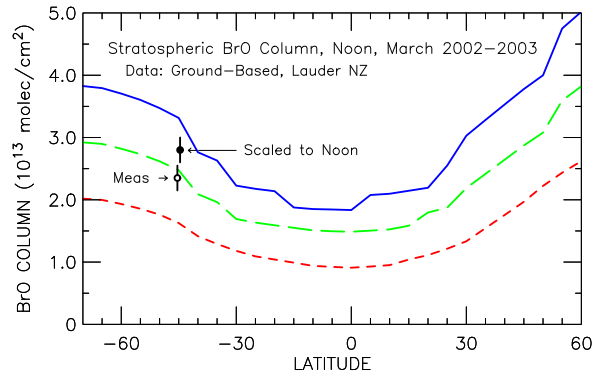


Figure 8. Stratospheric BrO vertical column measured over Lauder, New Zealand (45°S) at a solar zenith angle of 80° during March 2002 and March 2003 (open circle) reported by *Schofield et al.* [2004]. Data for the two years, which are quite similar, have been averaged. Error bar represents measurement uncertainty described by *Schofield et al.* [2004]. The closed circle represents the BrO vertical column at noon over Lauder. Calculated stratospheric BrO vertical column at noon from the AER 2D model (March 2003) is shown as a function of latitude for runs using values of $\text{Br}_y^{\text{TROP}}$ equal to 0 (red short-dashed), 4 (green long-dashed), and 8 (blue solid) ppt.

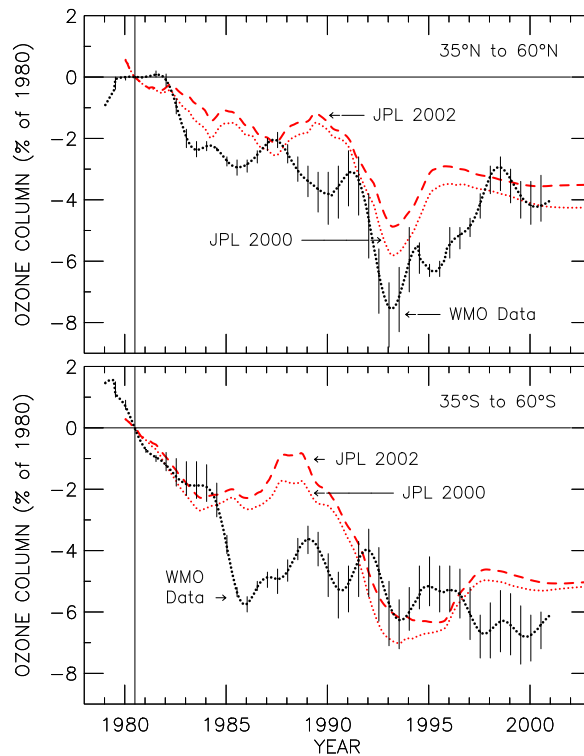


Figure 9. Calculated change in column ozone relative to 1980 levels for 35°N to 60°N (panel *a*) and for 35°S to 60°S (panel *b*) using the AER 2D model with $\text{Br}_y^{\text{TROP}}$ set equal to 0, using JPL 2002 (red dashed) and using JPL 2000 kinetics (red dotted). Also shown are the observed changes in column ozone, same data as presented in figure 4-33 of *WMO* [2003].

Table 1. Model Inputs for Calculation of Br_y from measured BrO, 22°S, 29 November 1997.

Alt (km)	T (K)	p (hPa)	BrO (ppt)	BrO Unc. Low (ppt)	BrO Unc. High (ppt)	SZA (deg)	O ₃ (ppm)	N ₂ O (ppb)	NO _y (ppb)	CH ₄ (ppm)	H ₂ O (ppm)	Sulfate SA 10 ⁻⁸ cm ² /cm ³
15	201.9	132.2	0.586	0.00	2.09	77.97	0.19	313.10	0.69	1.74	6.05	4.81
16	202.1	109.3	1.09	0.00	2.64	78.74	0.052	313.10	0.69	1.74	5.00	3.89
17	195.9	93.0	1.71	0.09	3.32	79.27	0.11	313.10	0.69	1.74	4.32	1.88
18	199.1	78.6	3.35	1.60	5.04	79.81	0.55	300.60	1.73	1.61	3.96	1.05
19	203.8	65.6	4.26	2.44	6.01	80.51	0.68	288.80	2.67	1.57	3.91	0.65
20	208.4	57.1	6.11	4.18	7.91	81.06	1.43	279.80	3.38	1.53	3.95	0.64
21	212.4	47.3	7.46	5.39	9.37	81.74	1.99	269.10	4.19	1.49	4.00	0.59
22	217.0	40.6	8.07	5.96	10.02	82.29	2.59	259.00	4.94	1.44	4.13	0.54
23	218.3	34.8	9.46	7.24	11.48	82.81	3.41	248.10	5.73	1.39	4.27	0.51
24	216.7	29.6	12.5	9.94	14.73	83.30	4.85	238.70	6.39	1.35	4.38	0.45
25	221.6	24.5	11.6	9.17	13.80	83.93	5.25	229.60	7.01	1.32	4.45	0.36
26	223.1	21.4	11.5	8.88	13.92	84.39	5.81	223.30	7.43	1.29	4.49	0.31
27	227.1	18.9	14.7	11.56	17.50	84.72	7.50	217.90	7.79	1.26	4.53	0.26
28	229.2	15.8	15.6	12.08	18.76	85.41	8.73	210.40	8.27	1.23	4.59	0.23
29	241.4	13.7	15.7	11.54	19.39	85.96	9.34	197.10	9.10	1.20	4.64	0.21
30	234.2	11.5	14.8	10.78	18.48	86.68	9.60	174.20	10.44	1.16	4.71	0.22

Table 2. Model Output: Calculated Br_y, 22°S, 29 November 1997, using inputs from Table 1.

Alt (km)	Br _y (ppt)	Br _y Meas. Unc. Low (ppt)	Br _y Meas. Unc. High (ppt)	Br _y Total Unc. Low (ppt)	Br _y Total Unc. High (ppt)
15	1.38	0.00	4.91	0.00	4.93
16	3.98	0.00	9.63	0.00	9.63
17	4.35	0.22	8.44	0.21	8.46
18	8.79	4.20	13.23	3.81	14.24
19	12.03	6.88	16.96	6.14	18.90
20	16.46	11.25	21.31	9.80	24.90
21	18.57	13.41	23.32	11.71	27.68
22	18.95	13.99	23.53	12.32	27.93
23	21.89	16.75	26.57	14.67	31.96
24	28.41	22.60	33.48	19.66	41.20
25	24.55	19.40	29.20	17.27	34.94
26	23.42	18.08	28.35	16.36	33.14
27	28.38	22.33	33.79	20.52	38.90
28	28.07	21.73	33.75	20.49	37.77
29	26.99	19.85	33.33	19.10	35.57
30	25.01	18.22	31.22	17.52	33.35

Table 3. Measured and Modeled Ozone Depletion,
percent of 1980 value
Time interval: start of 1980 to end of 2000
Model: AER 2D [*Rinsland et al.*, 2003]
Data: Merged satellite data [*WMO*, 2003]

35°–60°N:

Model:	$\text{Br}_y^{\text{TROP}}$	JPL 2002	JPL 2000
	0 ppt	-2.24	-2.69
	4 ppt	-2.70	-3.16
	8 ppt	-3.16	-3.63
Data:		-3.44	

35°–60°S:

Model:	$\text{Br}_y^{\text{TROP}}$	JPL 2002	JPL 2000
	0 ppt	-3.31	-3.75
	4 ppt	-3.73	-4.18
	8 ppt	-4.11	-4.58
Data:		-4.42	

End of Auxiliary Material, paper 2004GL021504